

## Controlling Crystallization, Mechanical Properties and Heat Resistance of Poly(L-lactide)-*b*-polyethylene glycol)-*b*-poly(L-lactide) Bioplastic by Melt Blending with Low Molecular Weight Poly(D-lactide)/Poly(L-lactide) Mixtures

YODTHONG BAIMARK\*<sup>ORCID</sup> and THEERAPHOL PHROMSOPHA<sup>ORCID</sup>

Biodegradable Polymers Research Unit, Department of Chemistry and Centre of Excellence for Innovation in Chemistry, Faculty of Science, Mahasarakham University, Mahasarakham 44150, Thailand

\*Corresponding author: Tel./Fax: +66 43 754246; E-mail: yodthong.b@msu.ac.th

Received: 18 February 2022;

Accepted: 20 May 2022;

Published online: 15 June 2022;

AJC-20866

The crystallization behaviour, mechanical properties and heat resistance were determined for mixtures of poly(L-lactide)-*b*-polyethylene glycol)-*b*-poly(L-lactide) (PLLA-PEG-PLLA) blended with poly(D-lactide)/poly(L-lactide) with *m.w.* of 6,000 g/mol (PDLA6k/PLLA6k). These blends were prepared by melt blending. PLLA-PEG-PLLA/PDLA6k/PLLA6k ratios of 90/10/0, 90/7.5/2.5, 90/5/5, 90/2.5/7.5 and 90/0/10 %wt. were investigated. PLLA-PEG-PLLA/PDLA6k and PLLA-PEG-PLLA/PLLA6k blends were also prepared for comparison. The presence of PDLA6k/PLLA6k mixture improved crystallization and heat resistance of PLLA-PEG-PLLA and this improvement was related to increased PDLA6k content. However, the 90/10/0 blend film was brittle but 90/7.5/2.5, 90/5/5, 90/2.5/7.5 and 90/0/10 blend films were not. The PLLA6k blending enhanced film flexibility. The results suggested that the PLLA-PEG-PLLA blends with controllable mechanical properties and heat resistance can be prepared by varying the PDLA6k/PLLA6k ratio for use as flexible and heat-resistant biodegradable bioplastics.

**Keywords:** Poly(lactic acid), Polyethylene glycol, Stereocomplex, Crystallization, Heat resistance.

### INTRODUCTION

Poly(L-lactic acid) or poly(L-lactide) (PLLA) has attracted extensive attention for use instead of traditional petroleum-based plastics to reduce plastic-waste pollution. This is due to PLLA being non-toxic, biocompatible, bio-renewable, biodegradable and easily processable [1-3]. Nevertheless, the drawbacks of PLLA, such as low flexibility and poor heat-resistance, have limited some applications such as hot-fill packaging, electrical devices and microwave applications, *etc.* [4-6].

PLLA-*b*-polyethylene glycol)-*b*-PLLA triblock copolymers (PLLA-PEG-PLLA) are biocompatible and biodegradable polymers that have been widely used in tissue engineering and drug delivery applications [7-9]. PLLA-PEG-PLLAs are flexible bioplastics because the PEG middle-blocks induce plasticizing effects leading to enhanced chain mobility of PLLA end-blocks [10-12]. Unfortunately, these flexible PLLA-PEG-PLLA still have poor heat-resistance [13].

Poly(L-lactic acid) (PLLA) with low crystallinity-content exhibited poor heat-resistance because of its poor stiffness at temperatures higher than its glassy-to-rubbery transition region [14,15]. Therefore, many researchers have reported on ways of increasing crystallinity-content of PLLA by development a nucleating effect [14-17]. It has been shown that stereocomplex-PLA crystallites obtained by PLLA and poly(D-lactide) (PDLA) blending accelerated crystallization of homo-PLLA due to stereocomplex crystallites acting as nucleating sites [18]. The stereocomplex-PLA crystallites had melting temperatures (210-240 °C) higher than homo-PLA crystallites (150-170 °C) due to stronger interactions between PLLA and PDLA chains [18-20]. PLLA and PDLA chains with lower molecular weight showed better stereocomplex formation [21,22]. In addition, low molecular weight PLLA has been used to accelerate crystallization of high molecular weight PLLA by enhancing its chain mobility [23-25]. However, low molecular weight PDLA and low molecular weight PLLA have not been blended together for improving crystallization of PLLA-PEG-PLLA.

Thus, the aim of this work was to investigate effects of low molecular weight PDLA/low molecular weight PLLA blends on crystallization behavior, mechanical properties and heat resistance of PLLA-PEG-PLLA. The PLLA-PEG-PLLA/low molecular weight PDLA and PLLA-PEG-PLLA/low molecular weight PLLA blends were also prepared for comparison.

## EXPERIMENTAL

Chain-extended PLLA-PEG-PLLA with a melt flow index (MFI) of 26 g/10 min (determined at 190 °C under 2.16 kg load) was synthesized by ring-opening polymerization of L-lactide monomer in bulk at 165 °C for 6 h under nitrogen atmosphere in the presence of 2.0 parts per hundred of resin (phr.) Joncryl® ADR4368 (chain extender) according to our previous work [26]. Stannous octoate and PEG (*m. w.* 20,000 g/mol) were used as the initiating system. Low molecular weight PDLA (PDLA6k) and low molecular weight PLLA (PLLA6k) were synthesized by ring-opening polymerization of L-lactide monomer in bulk at 165 °C for 2.5 h under nitrogen atmosphere as described in our previous work [27]. Stannous octoate and 1-dodecanol were used as the initiating system. Number-average molecular weight ( $M_n$ ) of PDLA6k and PLLA6k from gel permeation chromatography (GPC) were 5,700 and 6,200 g/mol, respectively. Their dispersity indices were 1.9 and 1.4, respectively.

**Preparation of PLLA-PEG-PLLA blends:** PLLA-PEG-PLLA, PDLA6k and PLLA6k were dried in a vacuum oven at 50 °C overnight before melt blending at 190 °C using a Rheomix batch mixer (HAAKE PolyLab OS) with a rotor speed of 100 rpm for 4 min. PLLA-PEG-PLLA/PDLA6k and PLLA-PEG-PLLA/PLLA6k blends were prepared with PDLA6k or PLLA6k ratios of 2.5, 5.0 and 10.0%wt. Blends with PLLA-PEG-PLLA/PDLA6k/PLLA6k ratios of 90/10/0, 90/7.5/2.5, 90/5/5, 90/2.5/7.5 and 90/0/10 %wt. were investigated. Pure PLLA-PEG-PLLA (100/0) was also prepared by the same method for comparison.

The blends were dried in a vacuum oven at 50 °C overnight before compression moulding. Blend films (100 mm × 100 mm × 0.2 mm) were fabricated using a compression moulding machine (Auto CH Carver) operated at 190 °C without any force for 3.0 min before compressing for 1.0 min under 2.5 MPa load. The obtained samples were then quenched to 25 °C with water-flow plate under 2.5 MPa load for 1.0 min.

**Characterization of PLLA-PEG-PLLA blends:** A differential scanning calorimeter (Perkin-Elmer Pyris Diamond) was used to study thermal transition properties of the blends under nitrogen gas flow. The blends were first heated at 200 °C for 3 min to remove their thermal history, then fast quenched before a heating scan from 0 °C to 200 °C at a rate of 10 °C/min to determine glass transition ( $T_g$ ), cold crystallization ( $T_{cc}$ ) and melting ( $T_m$ ) temperatures as well as enthalpies of melting ( $\Delta H_m$ ) and cold crystallization ( $\Delta H_{cc}$ ). The degree of crystallinity for homo-PLLA crystallites from DSC (DSC- $X_{c,hc}$ ) was calculated from following equation.

$$\text{DSC-}X_{c,hc} (\%) = \frac{[\Delta H_m - \Delta H_{cc}]}{93} \times 100 \quad (1)$$

where the 93 J/g is the  $\Delta H_m$  for 100% crystallinity content of PLLA [28,29].

The blends were melted at 200 °C for 3 min to remove their thermal history before a cooling scan from 200 °C to 0 °C at a rate of 10 °C/min to investigate their crystallization behaviours. Crystallization temperature ( $T_c$ ) was detected. For half of crystallization time ( $t_{1/2}$ ) measurement, the blends were first heated at 200 °C for 3 min to completely erase thermal history, then quenched to 120 °C at a rate of 50 °C/min and isothermally scanned at 120 °C until the completion of crystallization [30]. The  $t_{1/2}$  is the time required to obtain half of the final crystallinity content.

Crystalline characters of the blend films were investigated using a wide-angle X-ray diffractometer (XRD, Bruker D8 Advance) equipped with a copper tube operating at 40 kV and 40 mA producing  $\text{CuK}\alpha$  radiation. Scan speed was 3°/min. The degree of homo-PLA crystallinity (XRD- $X_{c,hc}$ ), degree of stereo-complex-PLA crystallinity (XRD- $X_{c,sc}$ ) and degree of total crystallinity (XRD- $X_c$ ) from XRD of the blends were calculated from eqns. 2, 3 and 4, respectively.

$$\text{XRD-}X_{c,hc} (\%) = \frac{A_{c,hc}}{A_{c,hc} + A_{c,sc} + A_a} \times 100 \quad (2)$$

$$\text{XRD-}X_{c,sc} (\%) = \frac{A_{c,sc}}{A_{c,hc} + A_{c,sc} + A_a} \times 100 \quad (3)$$

$$\text{XRD-}X_c (\%) = [\text{XRD-}X_{c,hc} + \text{XRD-}X_{c,sc}] \times 100 \quad (4)$$

where the  $A_{c,hc}$ ,  $A_{c,sc}$  and  $A_a$  are areas of XRD peaks for homo-PLA crystallites and stereocomplex-PLA crystallites as well as amorphous halo, respectively.

Tensile properties of the blend films were investigated using an universal mechanical testing machine (Liyi Environmental Technology LY-1066B) with a load cell of 100 kg, a crosshead speed of 50 mm/min and a gauge length of 50 mm. The film sizes were 100 mm × 10 mm. The averaged tensile properties were obtained from at least five measurements.

Dimensional stability to heat of the blend films was determined under a 200 g load in an air oven at 80 °C for 30 s with an initial gauge length of 20 mm. The film sizes were 40 mm × 5 mm. The dimensional stability to heat was calculated by eqn. 5 [13]:

$$\text{Dimensional stability to heat } (\%) = \frac{\text{Initial gauge length}}{\text{Final gauge length}} \times 100 \quad (5)$$

## RESULTS AND DISCUSSION

**Thermal transition properties:** Fig. 1 shows DSC heating curves of PLLA-PEG-PLLA blends. The results from DSC heating curves are summarized in Table-1. PDLA6k blending did not affect the glass-transition temperature ( $T_g$ ) of PLLA-PEG-PLLA matrices. Their  $T_g$  values were in range 33-34 °C. This may be due to PDLA6k chains being formed as stereo-complex crystallites with PLLA end-blocks of PLLA-PEG-PLLA [27]. In contrast,  $T_g$  of PLLA-PEG-PLLA/PLLA6k blends slightly decreased as the PLLA6k ratio increased. This may be explained by the PLLA6k chains induced plasticizing effect for PLLA-PEG-PLLA matrix [24,25]. Therefore,  $T_g$  of PLLA-PEG-PLLA/PDLA6k/PLLA6k blends decreased as the PLLA6k ratio increased.

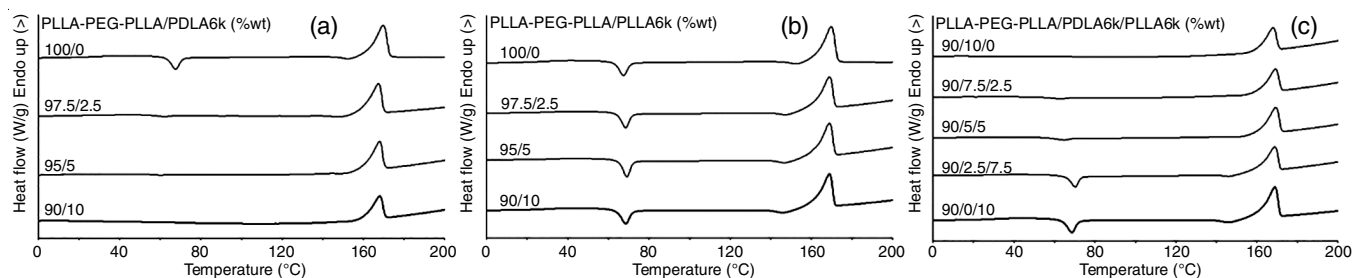


Fig. 1. DSC heating curves of PLLA-PEG-PLLA/PDLA6k, PLLA-PEG-PLLA/PLLA6k and PLLA-PEG-PLLA/PDLA6k/PLLA6k blends with various blend ratios

TABLE-1  
THERMAL TRANSITION PROPERTIES FROM DSC HEATING CURVES OF PLLA-PEG-PLLA BLENDS

PLLA-PEG-PLLA blends	$T_g$ (°C) <sup>a</sup>	$T_{cc}$ (°C) <sup>b</sup>	$T_m$ (°C) <sup>c</sup>	DSC- $X_{c,hc}$ (%) <sup>d</sup>
PLLA-PEG-PLLA/PDLA6k (%wt)				
100/0	33	68	170	35.2
97.5/2.5	33	62	168	44.8
95/5	33	60	168	39.7
90/10	34	–	168	32.4
PLLA-PEG-PLLA/PLLA6k (%wt)				
100/0	33	68	170	35.2
97.5/2.5	33	69	169	34.0
95/5	31	69	169	33.9
90/10	30	69	169	34.8
PLLA-PEG-PLLA/PDLA6k/PLLA6k (%wt)				
90/10/0	34	–	168	32.4
90/7.5/2.5	32	63	169	32.8
90/5/5	33	65	169	33.1
90/2.5/7.5	30	70	169	33.9
90/0/10	30	69	169	34.8

<sup>a</sup>Glass-transition temperature; <sup>b</sup>Cold-crystallization temperature; <sup>c</sup>Melting temperature; <sup>d</sup>Degree of crystallinity from DSC heating curves calculated from eqn. 1.

The  $T_{cc}$  peaks of the PLLA-PEG-PLLA/PDLA6k blends significantly shifted to lower temperature when the PDLA6k ratio was increased. The crystallites of stereocomplex PLA (scPLA) acted as nucleating sites for homo-PLA crystallization [18–20]. The  $T_{cc}$  peaks of PLLA-PEG-PLLA/PLLA6k did not shift by PLLA6k blending. However, the  $T_{cc}$  peaks of PLLA-PEG-PLLA/PDLA6k/PLLA6k blends shifted to higher temperature as the PLLA6k ratio increased because crystallinity content of scPLA decreased. All the PLLA-PEG-PLLA blends had  $T_m$  in range 168–170 °C.

Crystallization temperatures ( $T_c$ ) of PLLA-PEG-PLLA blends from DSC cooling curves are shown in Fig. 2. The  $T_c$  peaks of PLLA-PEG-PLLA/PDLA6k and PLLA-PEG-PLLA/PLLA6k blends were largely shifted and slightly shifted, respectively to higher temperature as the PDLA6k and PLLA6k ratios increased; this confirmed that crystallizability of PLLA-PEG-PLLA matrices can be improved by PDLA6k and PLLA6k blending (Table-2). It should be noted that PDLA6k blending was more effective for crystallization of PLLA end-blocks than was PLLA6k blending. The  $T_c$  peaks of PLLA-PEG-PLLA/PDLA6k/PLLA6k blends shifted to lower temperature when

TABLE-2  
THERMAL TRANSITION PROPERTIES FROM DSC COOLING AND DSC ISOTHERMAL CURVES OF PLLA-PEG-PLLA BLENDS

PLLA-PEG-PLLA blends	$T_c$ (°C) <sup>a</sup>	$t_{1/2}$ (min) <sup>b</sup>
PLLA-PEG-PLLA/PDLA6k (%wt)		
100/0	101	1.39
97.5/2.5	117	0.93
95/5	120	0.82
90/10	123	0.77
PLLA-PEG-PLLA/PLLA6k (%wt)		
100/0	101	1.39
97.5/2.5	102	1.10
95/5	103	1.06
90/10	105	1.02
PLLA-PEG-PLLA/PDLA6k/PLLA6k (%wt)		
90/10/0	123	0.77
90/7.5/2.5	124	0.89
90/5/5	124	0.94
90/2.5/7.5	118	0.97
90/0/10	105	1.02

<sup>a</sup>Crystallization temperature obtained from DSC cooling curves; <sup>b</sup>Half of crystallization time obtained from DSC isothermal curves

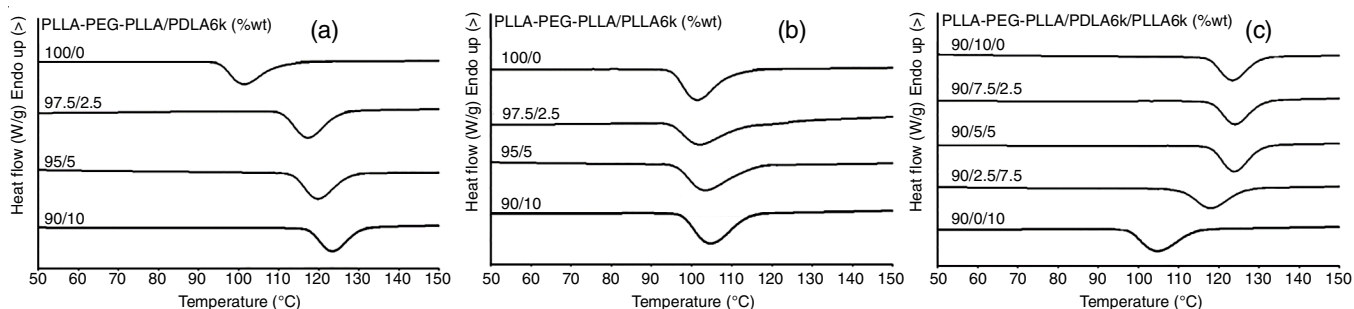


Fig. 2. DSC cooling curves of PLLA-PEG-PLLA/PDLA6k, PLLA-PEG-PLLA/PLLA6k and PLLA-PEG-PLLA/PDLA6k/PLLA6k blends with various blend ratios

the PLLA6k ratio was increased indicating that crystallizability of PLLA end-blocks during cooling scan was suppressed.

Half of crystallization times ( $t_{1/2}$ ) values from DSC isothermal curves are reported in Table-2. The shorter  $t_{1/2}$  values indicated faster crystallization. The  $t_{1/2}$  values of PLLA-PEG-PLLA/PDLA6k and PLLA-PEG-PLLA/PLLA6k blends dramatically decreased and slightly decreased, respectively as the PDLA6k and PLLA6k ratios increased, supporting a conclusion that PDLA6k and PLLA6k blending enhanced crystallization of PLLA-PEG-PLLA matrices (Fig. 3). The  $t_{1/2}$  values of PLLA-PEG-PLLA/PDLA6k/PLLA6k blends increased as the PLLA6k ratio increased.

The results from both the DSC cooling curves and DSC isothermal curves supported the conclusion that PDLA6k blending was more effective for the development of PLLA-PEG-PLLA crystallization than the PLLA6k blending, corresponding to the results from DSC heating curves. It can be concluded that the crystallization of PLLA-PEG-PLLA/PDLA6k/PLLA6k blends can be varied by adjusting the PDLA6k/PLLA6k ratio.

**Crystalline characters:** Crystalline characters of the blend films were investigated from XRD patterns as shown in Fig. 4. All degrees of crystallinity values from XRD of the blend films are summarized in Table-3. Pure PLLA-PEG-PLLA film displays a XRD diffraction peak at  $2\theta = 16.7^\circ$  corresponding to homo-PLA crystallites (hc) [29] with 11.2% XRD- $X_{c,hc}$ . PLLA-PEG-PLLA/PDLA6k blend films in Fig. 4a shows both peak types of hc at  $2\theta = 16.7^\circ$  and  $19.1^\circ$  [22,29] as well as of stereocomplex-PLA crystallites (sc) at  $2\theta = 11.9^\circ$ ,  $20.8^\circ$  and  $24.0^\circ$  [18,21,22]. All degrees of crystallinity including XRD- $X_{c,hc}$ , XRD- $X_{c,sc}$  and XRD- $X_c$  significantly increased as the PDLA6k ratio increased (Table-3). This may be explained by the higher PDLA6k ratio induced more stereocomplexation between PLLA and PDLA chains to increase the XRD- $X_{c,sc}$  [19,22]. Moreover, the obtained sc sites acted as nucleating

PLLA-PEG-PLLA blend films	XRD- $X_{c,hc}$ (%) <sup>a</sup>	XRD- $X_{c,sc}$ (%) <sup>b</sup>	XRD- $X_c$ (%) <sup>c</sup>
PLLA-PEG-PLLA/PDLA6k (%wt)			
100/0	11.2	-	11.2
97.5/2.5	11.8	4.3	16.1
95/5	14.6	10.7	25.3
90/10	15.4	23.2	38.6
PLLA-PEG-PLLA/PLLA6k (%wt)			
100/0	11.2	-	11.2
97.5/2.5	12.0	-	12.0
95/5	11.1	-	11.1
90/10	10.7	-	10.7
PLLA-PEG-PLLA/PDLA6k/PLLA6k (%wt)			
90/10/0	15.4	23.2	38.6
90/7.5/2.5	11.0	17.4	28.4
90/5/5	10.9	10.5	21.4
90/2.5/7.5	10.3	5.3	15.6
90/0/10	10.7	-	10.7

<sup>a</sup>Degree of homo-PLA crystallinity calculated from eqn. 2.  
<sup>b</sup>Degree of stereocomplex-PLA crystallinity calculated from eqn. 3.  
<sup>c</sup>Degree of total crystallinity calculated from eqn. 4.

sites for homo-PLA crystallization to increase the XRD- $X_{c,hc}$  [19].

For PLLA-PEG-PLLA/PLLA6k blend films in Fig. 4, all blend films exhibited only a peak of hc type at  $2\theta = 16.7^\circ$ . The XRD- $X_{c,hc}$  of PLLA-PEG-PLLA/PLLA6k blend films were in the range 10.7-12.0% that did not change significantly when the PLLA6k ratio was increased. Both the hc and sc peaks were detected for PLLA-PEG-PLLA/PDLA6k/PLLA6k blend films as presented in Fig. 4c. Their XRD- $X_{c,hc}$ , XRD- $X_{c,sc}$  and XRD- $X_c$  values trended to reduce as the PDLA6k ratio decreased. This was due to the XRD- $X_{c,sc}$  reducing as the PDLA6k ratio decreased.

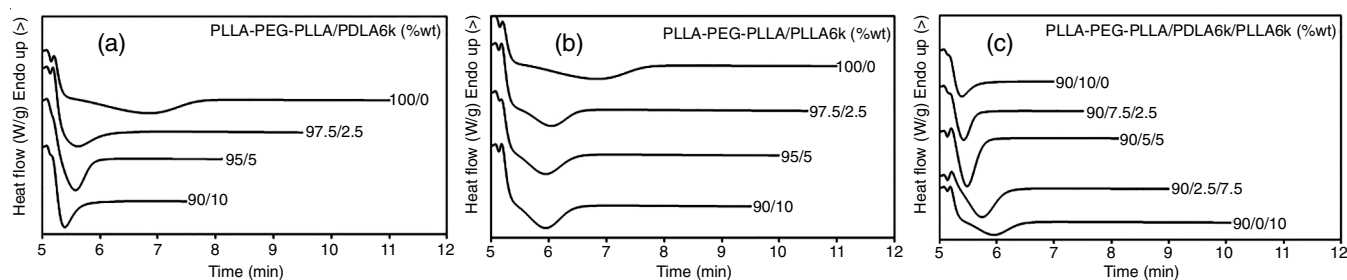


Fig. 3. DSC isothermal curves at 120 °C of PLLA-PEG-PLLA/PDLA6k, PLLA-PEG-PLLA/PLLA6k and PLLA-PEG-PLLA/PDLA6k/PLLA6k blends with various blend ratios

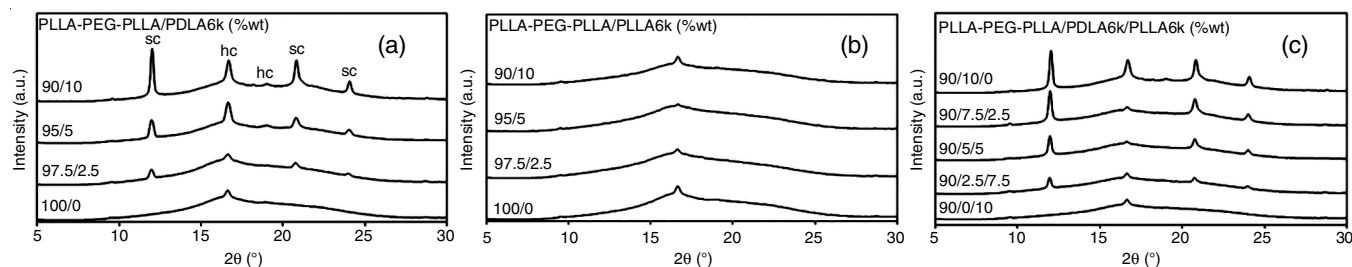


Fig. 4. XRD patterns of PLLA-PEG-PLLA/PDLA6k, PLLA-PEG-PLLA/PLLA6k and PLLA-PEG-PLLA/PDLA6k/PLLA6k blend films with various blend ratios

**Tensile properties:** Fig. 5 shows selected tensile curves of the blend films. The averaged tensile properties are shown in Table-4. The ultimate tensile stress, strain at break and Young’s modulus of pure PLLA-PEG-PLLA film in this work were 17.9 MPa, 343% and 237 MPa, respectively. The ultimate tensile stress and Young’s modulus of PLLA-PEG-PLLA/PDLA6k blend films slightly decreased and strain at break dramatically decreased as the PDLA6k ratio increased as illustrated in Fig. 5a. The 90/10 PLLA-PEG-PLLA/PDLA6k blend film exhibited a brittle character. This may have been due to the blend films with higher XRD- $X_c$  exhibiting smaller film-extensibility (Table-4) [22]. However, tensile properties of PLLA-PEG-PLLA films did not significantly change by PLLA6k blending as shown in Fig. 5b. This may be explained by their XRD- $X_c$  values being similar (10.7-12.0%). For the PLLA-PEG-PLLA/PDLA6k/PLLA6k blend films in Fig. 5c, ultimate tensile stress, Young’s modulus and strain at break significantly increased with the PLLA6k ratio. Flexibility of these blend films was then improved by increasing the PLLA6k ratio. This was due to the XRD- $X_c$  of blend films was suppressed.

**Heat resistance:** Dimensional stability to heat of film samples was used to determine heat resistance of blend films. The film samples were kept in an air oven at 80 °C under a 200 g hung load for 30 s to observe film extension. Good heat resistant polypropylene film prepared by the same method did not extend after test indicated that it had 100% dimensional stability to heat. The longer film-extension after test was assigned to lower dimensional stability to heat (lower heat-resistance) of the films [13].

Fig. 6 presents results of dimensional stability to heat of the blend films. The dimensional stability to heat of PLLA-

PLLA-PEG-PLLA blend films	Ultimate tensile stress (MPa)	Elongation at break (%)	Young’s modulus (MPa)
PLLA-PEG-PLLA/PDLA6k (%wt)			
100/0	17.9 ± 0.5	343 ± 40	237 ± 10
97.5/2.5	16.5 ± 1.1	241 ± 19	210 ± 29
95/5	16.9 ± 1.9	43 ± 6	219 ± 10
90/10	14.6 ± 0.6	4 ± 1	202 ± 19
PLLA-PEG-PLLA/PLLA6k (%wt)			
100/0	17.9 ± 0.5	393 ± 40	237 ± 10
97.5/2.5	19.2 ± 0.8	379 ± 18	228 ± 17
95/5	18.7 ± 1.5	418 ± 37	171 ± 20
90/10	20.8 ± 1.2	467 ± 42	210 ± 12
PLLA-PEG-PLLA/PDLA6k/PLLA6k (%wt)			
90/10/0	14.6 ± 0.6	4 ± 1	202 ± 19
90/7.5/2.5	17.8 ± 0.7	140 ± 15	229 ± 11
90/5/5	19.3 ± 1.0	255 ± 28	216 ± 27
90/2.5/7.5	19.4 ± 1.8	294 ± 34	239 ± 41
90/0/10	20.8 ± 1.2	467 ± 42	210 ± 12

PEG-PLLA/PDLA6k blend films in Fig. 6a steadily increased with the PDLA6k ratio suggesting that PDLA6k blending enhanced heat resistance of PLLA-PEG-PLLA films. The crystallinity content enhanced film stiffness to resist film deformation from heat [13,27], whereas PLLA6k blending reduced dimensional stability to heat of the PLLA-PEG-PLLA film. This may have been due to a plasticizing effect of PLLA6k to decrease film stiffness [25,26]. The dimensional stability to heat of PLLA-PEG-PLLA/PDLA6k/PLLA6k blend films in

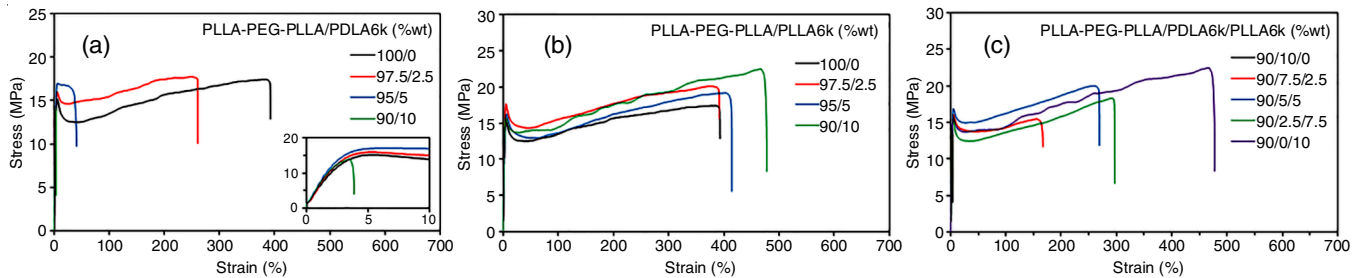


Fig. 5. Selected tensile curves of PLLA-PEG-PLLA/PDLA6k, PLLA-PEG-PLLA/PLLA6k and PLLA-PEG-PLLA/PDLA6k/PLLA6k blends with various blend ratios

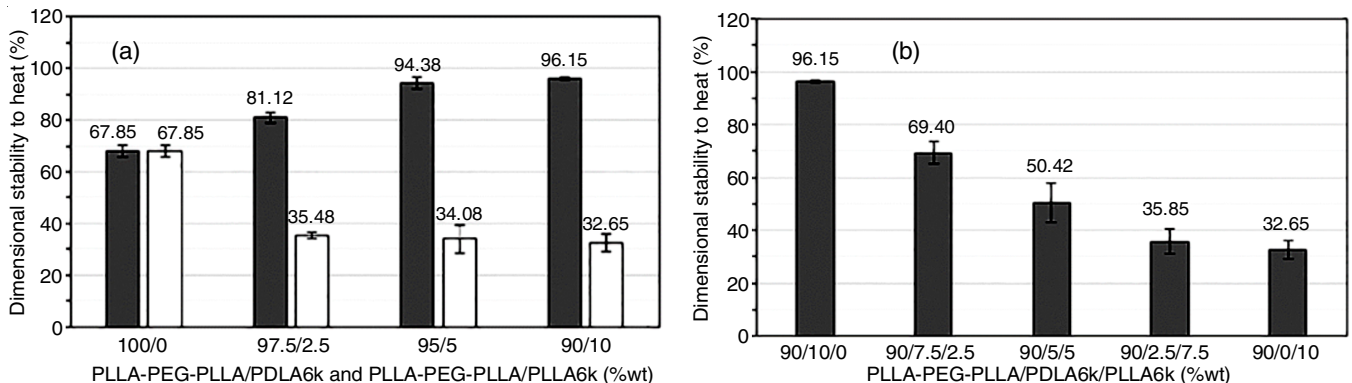


Fig. 6. Dimensional stability to heat of (a) PLLA-PEG-PLLA/PDLA6k (■) and PLLA-PEG-PLLA/PLLA6k (□) as well as (b) PLLA-PEG-PLLA/PDLA6k/PLLA6k blends with various blend ratios

Fig. 6b steadily decreased as the PLLA6k ratio increased. This was due to the XRD- $X_c$  of blend films decreasing as the PLLA6k ratio increased.

## Conclusion

The mixtures of poly(L-lactide)-*b*-polyethylene glycol-*b*-poly(L-lactide) (PLLA-PEG-PLLA) blended with poly(D-lactide)/poly(L-lactide) *viz.* PLLA-PEG-PLLA/PDLA6k, PLLA-PEG-PLLA/PLLA6k and PLLA-PEG-PLLA/PDLA6k/PLLA6k blends were prepared by melt blending. The influence of blend ratio on the crystallization, mechanical properties and heat resistance of the blends was determined. These properties of the PLLA-PEG-PLLA/PDLA6k/PLLA6k blends strongly depended upon the PDLA6k/PLLA6k ratio. The crystallizability, crystallinity content and heat resistance of PLLA-PEG-PLLA matrices was directly related to PDLA6k content as revealed by DSC, XRD and dimensional stability to heat, respectively. Also, PLLA6k blending improved flexibility of the blend films as determined by tensile tests. It is, therefore, concluded that the crystallizability, mechanical properties and heat resistance of PLLA-PEG-PLLA blend films can be tailored by adjusting the PDLA6k/PLLA6k ratio. These PLLA-PEG-PLLA blend films with controllable crystallizability, mechanical properties and heat resistance could be applied for use as high performance bioplastics.

## ACKNOWLEDGEMENTS

This research project was financially supported by Mahasarakham University, Mahasarakham, Thailand. One of the authors, YB is also grateful to the partially support provided by the Office of National Higher Education Science Research and Innovation Policy Council (NXPO), Thailand.

## CONFLICT OF INTEREST

The authors declare that there is no conflict of interests regarding the publication of this article.

## REFERENCES

- E. Castro-Aguirre, R. Auras, S. Selke, M. Rubino and T. Marsh, *Polym. Degrad. Stab.*, **154**, 46 (2018); <https://doi.org/10.1016/j.polymdegradstab.2018.05.017>
- D. da Silva, M. Kaduri, M. Poley, O. Adir, N. Krinsky, J. Shainsky-Roitman and A. Schroeder, *Chem. Eng. J.*, **340**, 9 (2018); <https://doi.org/10.1016/j.cej.2018.01.010>
- G. Li, M. Zhao, F. Xu, B. Yang, X. Li, X. Meng, L. Teng, F. Sun and Y. Li, *Molecules*, **25**, 5023 (2020); <https://doi.org/10.3390/molecules25215023>
- L. Quiles-Carrillo, M.M. Blanes-Martínez, N. Montanes, O. Fenollar, S. Torres-Giner and R. Balart, *Eur. Polym. J.*, **98**, 402 (2018); <https://doi.org/10.1016/j.eurpolymj.2017.11.039>
- N. Peelman, P. Ragaert, K. Ragaert, M. Erkoç, W. Van Brempt, F. Faelens, F. Devlieghere, B. De Meulenaer and L. Cardon, *Polym. Eng. Sci.*, **58**, 513 (2018); <https://doi.org/10.1002/pen.24760>
- F.L. Jin, R.R. Hu and S.J. Park, *Compos. B Eng.*, **164**, 287 (2019); <https://doi.org/10.1016/j.compositesb.2018.10.078>
- A. Basu, K.R. Kunduru, S. Doppalapudi, A.J. Domb and W. Khan, *Adv. Drug Deliv. Rev.*, **107**, 192 (2016); <https://doi.org/10.1016/j.addr.2016.07.004>
- H. Danafar, K. Rostamizadeh, S. Davaran and M. Hamidi, *Pharm. Dev. Technol.*, **22**, 947 (2017); <https://doi.org/10.3109/10837450.2015.1125920>
- T. Narancic, F. Cerrone, N. Beagan and K.E. O'Connor, *Polymers*, **12**, 920 (2020); <https://doi.org/10.3390/polym12040920>
- X. Yun, X. Li, Y. Jin, W. Sun and T. Dong, *Polym. Sci. Ser. A*, **60**, 141 (2018); <https://doi.org/10.1134/S0965545X18020141>
- Y. Baimark, W. Rungseesantivanon and N. Prakymoramas, *Mater. Des.*, **154**, 73 (2018); <https://doi.org/10.1016/j.matdes.2018.05.028>
- Y. Baimark and Y. Srisuwan, *J. Elastomers Plast.*, **52**, 142 (2020); <https://doi.org/10.1177/0095244319827993>
- S. Pasee and Y. Baimark, *Adv. Polym. Technol.*, **2019**, 8690650 (2019); <https://doi.org/10.1155/2019/8690650>
- X. Zhang, L. Meng, G. Li, N. Liang, J. Zhang, Z. Zhu and R. Wang, *J. Appl. Polym. Sci.*, **133**, 42999 (2016); <https://doi.org/10.1002/app.42999>
- R. Vadori, A.K. Mohanty and M. Misra, *Macromol. Mater. Eng.*, **298**, 981 (2013); <https://doi.org/10.1002/mame.201200274>
- S. Saeidlou, M.A. Huneault, H. Li and C.B. Park, *Prog. Polym. Sci.*, **37**, 1657 (2012); <https://doi.org/10.1016/j.progpolymsci.2012.07.005>
- D. Battezzore, S. Bocchini and A. Frache, *Express Polym. Lett.*, **5**, 849 (2011); <https://doi.org/10.3144/expresspolymlett.2011.84>
- X. Shi, Z. Jing and G. Zhang, *J. Polym. Res.*, **25**, 71 (2018); <https://doi.org/10.1007/s10965-018-1467-9>
- H. Tsuji, *Adv. Drug Deliv. Rev.*, **107**, 97 (2016); <https://doi.org/10.1016/j.addr.2016.04.017>
- E. El-Khodary, Y. Fukui, M. Yamamoto and H. Yamane, *J. Appl. Polym. Sci.*, **134**, 45489 (2017); <https://doi.org/10.1002/app.45489>
- J. Shao, S. Xiang, X. Bian, J. Sun, G. Li and X. Chen, *Ind. Eng. Chem. Res.*, **54**, 2246 (2015); <https://doi.org/10.1021/ie504484b>
- Y. Srisuwan and Y. Baimark, *E-Polymers*, **18**, 485 (2018); <https://doi.org/10.1515/epoly-2018-0115>
- N. Burgos, D. Tolaguera, S. Fiori and A. Jiménez, *J. Polym. Environ.*, **22**, 227 (2014); <https://doi.org/10.1007/s10924-013-0628-5>
- R. Avolio, R. Castaldo, G. Gentile, V. Ambrogi, S. Fiori, M. Avella, M. Cocca and M.E. Errico, *Eur. Polym. J.*, **66**, 533 (2015); <https://doi.org/10.1016/j.eurpolymj.2015.02.040>
- M.L. Di Lorenzo and R. Androsch, *Eur. Polym. J.*, **100**, 172 (2018); <https://doi.org/10.1016/j.eurpolymj.2018.01.030>
- Y. Baimark, W. Rungseesantivanon and N. Prakymoramas, *E-Polymers*, **20**, 423 (2020); <https://doi.org/10.1515/epoly-2020-0047>
- Y. Baimark, S. Pasee, W. Rungseesantivanon and N. Prakymoramas, *J. Polym. Res.*, **26**, 218 (2019); <https://doi.org/10.1007/s10965-019-1881-7>
- F.A. Syamani, Y.D. Kurniawan and L. Suryanegara, *Asian J. Chem.*, **30**, 1435 (2018); <https://doi.org/10.14233/ajchem.2018.21119>
- J. Jirum and Y. Baimark, *Asian J. Chem.*, **33**, 2135 (2021); <https://doi.org/10.14233/ajchem.2021.23299>
- L. Li, Z.Q. Cao, R.Y. Bao, B.H. Xie, M.B. Yang and W. Yang, *Eur. Polym. J.*, **97**, 272 (2017); <https://doi.org/10.1016/j.eurpolymj.2017.10.025>